Kobe University Repository : Kernel

PDF issue: 2026-11-20

Vibronic Trimer Design Enhancing Intramolecular Triplet-Exciton Hopping to Accelerate Triplet-Triplet Annihilation for Photon Upconversion

Higashi, Kousuke ; Okamoto, Tsubasa ; Iwaya, Nanami ; Sakuda, Eri ; Kay, Christopher W. M. ; Ikoma, Tadaaki ; Higashi, Masahiro ; Kobori,…

(Citation)
Angewandte Chemie International Edition,64(30):e202503846

(Issue Date)
2025-07-21

(Resource Type)
journal article

(Version)
Version of Record

(Rights)
© 2025 The Author(s). Angewandte Chemie International Edition published by Wiley-VCH GmbH
This is an open access article under the terms of the Creative Commons Attribution-NonCommercial-NoDerivs License, which permits use and distribution in any medium,…

(URL)
https://hdl.handle.net/20.500.14094/0100496029

KOBE UNIVERSITY

GDCh Research Article Angewandte International Edition Chemie www.angewandte.org

How to cite: *Angew. Chem. Int. Ed.* **2025**, e202503846
doi.org/10.1002/anie.202503846

Photon Upconversion

Vibronic Trimer Design Enhancing Intramolecular Triplet-Exciton Hopping to Accelerate Triplet-Triplet Annihilation for Photon Upconversion

Kousuke Higashi, Tsubasa Okamoto, Nanami Iwaya, Eri Sakuda, Christopher W. M. Kay, Tadaaki Ikoma, Masahiro Higashi, and Yasuhiro Kobori**

Abstract: Photon upconversion via triplet-triplet annihilation (TTA-UC) is a well-known process that converts low-energy light into higher-energy light. This process has attracted attention for its potential in various fields, including light-emitting devices, power generation and medical applications. It is desirable to develop TTA-UC materials of TTA emitters with large TTA rate constants (k_{TTA}). However, molecular design to accelerate the bimolecular rate constant of k_{TTA} has not been considered. We present a strategy to manipulate k_{TTA} by assembling multiple chromophores linked to a boron in a rotationally symmetric manner, causing asymmetric motions by a localized triplet exciton. We have studied tri(9-anthryl)borane, which consists of three anthracenes linked via boron, as a TTA emitter. Time-resolved luminescence measurements confirmed that k_{TTA} is improved compared to the conventional TTA-UC system using DPA, an anthracene-based monomer. Time-resolved electron paramagnetic resonance measurements showed that the improvement in k_{TTA} is due to fast intramolecular triplet exciton hopping coupled with vibrational motions in the trimer molecule, which extends the reactivity at the collision distance between the excitons through the pseudo-rotational motions. This molecular design that enhances TTA reactivity is expected to contribute to the future development of TTA-UC materials for sensing fluid environment.

Introduction

As a means to effectively utilize limited energy resources, light energy conversion technology is an indispensable element in modern society. Among them, photon upconversion via triplet-triplet annihilation (TTA-UC) is a chemical reaction process that converts two photons into one higher-energy photon.[1,2] This process operates even when incoherent low-intensity light is incident, making it possible to effectively utilize light of various wavelengths contained in sunlight. Therefore, TTA-UC attracts attention as a promising means to improve the light energy conversion efficiency in organic solar cells[3,4] and photocatalysis.[5,6] Furthermore, because TTA-UC can realize the light-energy conversion using weak excitation lights compatible with the human body, it is expected to be useful in various medical fields.[7–12] A typical

[*] K. Higashi, Dr. T. Okamoto, Prof. Dr. Y. Kobori
Department of Chemistry, Graduate School of Science, Kobe University, 1–1 Rokkodai–cho, Nada–ku, Kobe 657–8501, Japan
E-mail: okamoto.tsubasa.gp@u.tsukuba.ac.jp
ykobori@kitty.kobe-u.ac.jp

Dr. T. Okamoto, Prof. Dr. Y. Kobori
Molecular Photoscience Research Center, Kobe University, 1–1 Rokkodai–cho, Nada–ku, Kobe 657–8501, Japan

N. Iwaya, Prof. Dr. T. Ikoma
Graduate School of Science and Technology, Niigata University, Nishi-ku, Niigata 950–2181, Japan

Prof. Dr. E. Sakuda
Division of Chemistry and Materials Science, Integrated Science and Technology, Nagasaki University, Bunkyo-machi, Nagasaki 852–8521, Japan

Prof. Dr. C. W. M. Kay
Physical Chemistry and Chemistry Education, Saarland University, D-66123 Saarbrücken, Germany

Prof. Dr. C. W. M. Kay
London Centre for Nanotechnology, University of College London, 17–19 Gordon Street, London WC1H 0AH, United Kingdom

Prof. Dr. T. Ikoma
Center for Coordination of Research Facilities, Niigata University, Nishi-ku, Niigata 950–2181, Japan

Prof. Dr. M. Higashi
Department of Complex Systems Science, Graduate School of Informatics, Nagoya University, Furo-cho, Chikusa-ku, Nagoya 464–8601, Japan

Prof. Dr. Y. Kobori
CREST, JST, Honcho 4-1-8, Kawaguchi, Saitama 332-0012, Japan

Dr. T. Okamoto
Present address: Department of Materials Science, Institute of Pure and Applied Sciences and Research Center for Organic-Inorganic Quantum Spin Science and Technology, University of Tsukuba, 1-1-1 Tennodai, Tsukuba 305-8573, Japan

Additional supporting information can be found online in the Supporting Information section

© 2025 The Author(s). Angewandte Chemie International Edition published by Wiley-VCH GmbH. This is an open access article under the terms of the Creative Commons Attribution-NonCommercial-NoDerivs License, which permits use and distribution in any medium, provided the original work is properly cited, the use is non-commercial and no modifications or adaptations are made.

© 2025 The Author(s). Angewandte Chemie International Edition published by Wiley-VCH GmbH

TTA-UC system often consists of a combination of a sensitizer and an TTA emitter molecule and goes through a complex process.[13] TTA is a bimolecular reaction whereby two triplet-excitons collide. Hence the longer the lifetime (τ_T) of the triplet-exciton and the larger the TTA reaction rate (k_{TTA}), the higher the quantum yields (Φ_{TTA}) of TTA becomes. A conventional approach to prolong τ_T is to control the molecular structure to suppress nonradiative deactivation and excimer formation processes.[14–17]

For example, 9,10-diphenylanthracene (DPA), which is used as an TTA emitter in the TTA-UC systems, has very long τ_T, over 1 ms,[18] and achieves high Φ_{TTA}. On the other hand, molecular design focusing to improve the k_{TTA} is also important but has not been paid significant attention. When we only consider intramolecular TTA,[19–21] we do not need to discuss diffusion rate because the collisions between chromophore molecules are not needed for TTA. However, molecular diffusion is often required for several practical TTA-UC applications in fluid environments.

To increase k_{TTA} in the solution-based TTA-UC, it is necessary to either increase the diffusion rate of the emitter molecule or to enhance the effective TTA reaction zone between the triplet-excitons, that is, the spatial extent of unpaired orbitals in the triplet-exciton. Solution TTA-UC materials using low-viscosity solvents such as toluene and tetrahydrofuran have been reported in numerous studies.[15,20,22–24] When the molecular diffusion rate is larger than k_{TTA}, it is important to enhance the reactivity between the triplet excitons for improving k_{TTA}.[15,25,26] When k_{TTA} is the diffusion-controlled rate constant, it might be better to use a lower viscosity solvent, but will be difficult to find a solvent that can dramatically improve k_{TTA}. Enhancing the TTA reaction distance would be plausible when triplet-excitons possesses highly delocalized unpaired orbitals. However, this simple expansion of the orbitals generally lowers the triplet energy level, causing difficulty in obtaining the radiative first excited singlet state (S_1^{emi}) from the two of the first excited triplet states (T_1) as in the case of triplet-pair by pentacene, which is well known as a singlet-fission material.

Instead, if we can prepare a molecule containing multiple chromophores with a small core structure that has high rotational symmetry, we can expect to realize a situation where the triplet-exciton moves quickly between chromophores in the entire molecule by a pseudo-rotation caused by the dynamic Jahn-Teller effect in highly symmetric molecules such as fullerenes.[27–31] Thus, it is expected that the unpaired orbitals in the triplet-exciton can be equivalent to be delocalized during the time scale of the bimolecular triplet-triplet encounter by the collision without lowering the triplet energy, thereby improving k_{TTA}.[32–34]

For this, one needs to control the molecular motion by selecting the central atom bridging the chromophores. For example, Crystal Violet (CV) is a trimer with aniline chromophores linked by a central carbon that satisfies the octet rule. CV shows strong charge-transfer (CT) characteristics and takes on a stable planar structure in the triplet state.[35] On the other hand, in the case of bulky trimeric chromophores linked with a boron atom, the octet rule is not satisfied. This instability by the low bond-order

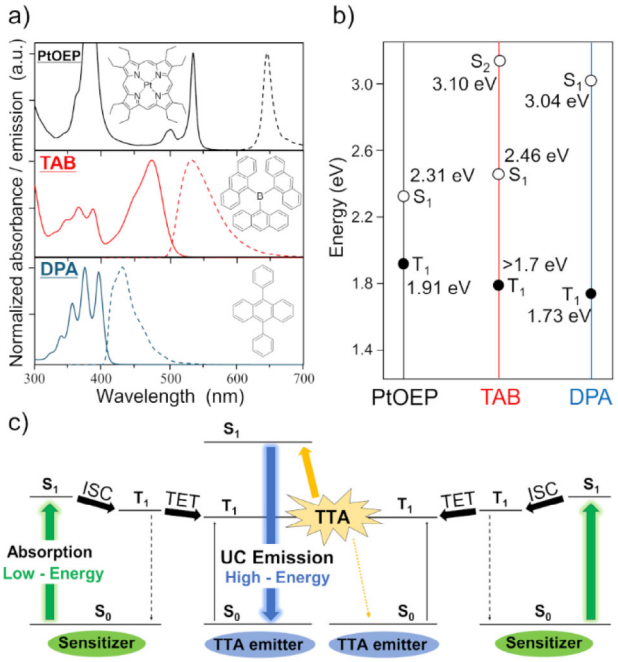


Figure 1. a) Absorption (solid lines) and emission (dotted lines) spectra of PtOEP (top), TAB (middle), and DPA (bottom) in toluene. The structure of each molecule is also shown. The emission spectrum around 646 nm of PtOEP is phosphorescence. Wavelengths of the excitation light are 530 nm for PtOEP, 350 nm for TAB and 300 nm for DPA, respectively. b) Energy levels of S_1, S_2 and T_1 states. c) Jablonski diagram of the TTA-UC process.

from the B atom is expected to lead to the molecular activation motions such as pseudo-rotation of triplet excitons within the trimer. To prove the concept of the above-mentioned strategy to improve k_{TTA}, we have employed a TTA-UC material of tri(9-anthryl)borane (TAB),[36,37] which is a trimer-type fluorescent molecule that is expected to exhibit triplet-exciton hopping within the molecule with the addition of the photosensitizer, platinum 2,3,7,8,12,13,17,18-octaethylporphyrin (PtOEP).[17,20–21] The TTA-UC emission from TAB is investigated by time-resolved fluorescence measurement to determine k_{TTA} in the PtOEP/TAB system. The estimated k_{TTA} value is compared with that in PtOEP/DPA system, which is well known for its high overall UC quantum yield ($\Phi_{UC} \approx 24\%$),[20,38] to verify the effect of exciton dynamics by the trimerization on k_{TTA}. Furthermore, the electronic structure of the triplet-exciton generated in TAB is investigated by using time-resolved electron paramagnetic resonance (TREPR), and it is clarified from a molecular point of view how the molecular structure and mobility contribute to the improvement of k_{TTA}.

Results and Discussion

To characterize excited state energies, Figure 1a shows the absorption and emission spectra of PtOEP, TAB, and DPA along with their molecular structures. TAB has a unique structure with three anthracenes linked via boron in a three-dimensionally orthogonal arrangement. TAB was synthesized

© 2025 The Author(s). Angewandte Chemie International Edition published by Wiley-VCH GmbH

15213773, 0, Downloaded from https://onlinelibrary.wiley.com/doi/10.1002/anie.202503846 by Kobe University, Wiley Online Library on [09/06/2025]. See the Terms and Conditions (https://onlinelibrary.wiley.com/terms-and-conditions) on Wiley Online Library for rules of use; OA articles are governed by the applicable Creative Commons License

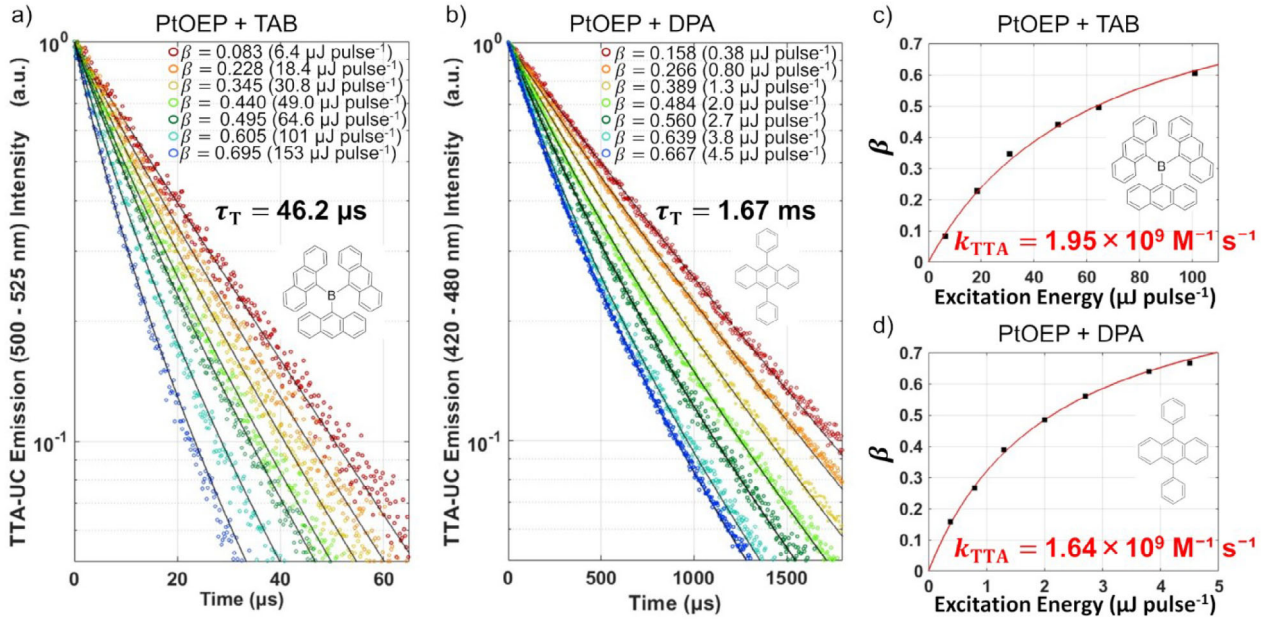


Figure 2. Time-resolved upconverted emission of a) 60 μM PtOEP/1.2 mM TAB system and b) 60 μM PtOEP/1.2 mM DPA system in toluene at 298 K. Emission was measured at (a) 490–520 nm and (b) 420–480 nm, respectively, upon pulsed excitation at 532 nm. The solid curves (black) represent best fits according to Equation (1). c, d) Dependences of β on the fluence of incident light energy. $k_{TTA} = 1.95(\pm0.04) \times 10^9$ $M^{-1}s^{-1}$ and $1.64(\pm0.02) \times 10^9$ $M^{-1}s^{-1}$ for the (c) PtOEP/TAB and (d) PtOEP/DPA systems, respectively, were determined according to Equation (2).

by a previously reported method.[37] Due to the interaction between the three anthracene moieties, the absorption and fluorescence wavelengths of TAB are red-shifted compared to DPA, which is one of the anthracene monomer derivatives. This is ascribed to a CT type transition between HOMO and LUMO as shown by the DFT calculation in Figure S1.

Figure 1b shows the energy levels of the first excited singlet state (S_1) and the first excited triplet state (T_1) of each molecule. The S_1 and T_1 energies of PtOEP shown in Figure 1b are based on reported values.[39] PtOEP absorbs green light and exhibits a high ISC yield ($\Phi_{ISC} \approx 1$) due to the heavy atom effect,[40] making its energy relationship with anthracene derivatives suitable for the TTA-UC system. The S_1 energies of TAB and DPA were estimated from the intersection of the absorption and fluorescence spectra in Figure 1a, which is consistent with a TD-SCF calculation (Figure S1). The S_2 energy of TAB was estimated from the edge of the short-wavelength absorption band (400 nm). The T_1 energies of TAB (>1.7 eV) and DPA (1.73 eV) were estimated based upon the TTA-UC observation via TTE from TAB to DPA (Figure S2). For DPA, the calculated T_1 energy[20] coincided with experimentally determined value.[41] From Figure 1b, the TTA is expected to proceed from the T_1T_1 pair (reactant energy: > 3.4 eV) to the S_1S_0 state (product energy: 2.46 eV) in TAB.

Figure 1c shows the Jablonski diagram of the TTA-UC system composed of two photosensitizers and two emitters. The T_1 energy of PtOEP is higher than those of DPA and TAB, indicating that the TET reactions from PtOEP to DPA or TAB occur exothermically. Additionally, because the S_1 energies of DPA and TAB are lower than twice of their respective T_1 energies, the energy requirements of TTA-UC are satisfied when both DPA and TAB are used as the TTA emitters. Compared to the TTA-UC material composed of PtOEP and DPA, the PtOEP/TAB system exhibits a smaller anti-Stokes shift. This is because the orbital distributions of HOMO and LUMO in the TAB molecule extend over two or three anthracene moieties via the boron atom (Figure S1) to cause a CT character, resulting in a lowered S_1 energy level.

To determine TTA rate constants, the photon upconversion processes of the two different TTA emitters were examined using time-resolved photoluminescence measurements at room temperature. Solutions consisting of 60 μM PtOEP and 1.2 mM TAB or DPA were prepared in toluene and were degassed by freeze-pump-thaw cycles. Figure 2a and b show the time profiles of the TTA-UC emission intensities for the PtOEP/TAB and PtOEP/DPA systems, respectively, detected after excitation by laser pulse at 532 nm at various intensities. In both systems, as the excitation light intensity increases, the emission decays faster, indicating that the emission occurs through a bimolecular reaction process as illustrated in the Figure 1c.

To analyze the time profiles of TTA-UC emission under different excitation intensities,[20,42] we used a method detailed in the Supporting Information with Figure S3 and Table S1. The τ_T and the dimensionless parameter of β (Equation 2) are obtained from the time-dependent UC emission intensity, $I_{UC}(t)$[43,44]:

$$I_{UC}(t) \propto \left([^3Emi^*]_0 \frac{1-\beta}{\exp\left(\frac{t}{\tau_T}\right) - \beta} \right)^2 \quad (1)$$

$[^3Emi^*]_0$ produced by the TET ($t = 0$) was estimated from the incident light intensity and the photophysical parameters of PtOEP. Solid black curves in Figure 2a and b show the

© 2025 The Author(s). Angewandte Chemie International Edition published by Wiley-VCH GmbH

15213773, 0, Downloaded from https://onlinelibrary.wiley.com/doi/10.1002/anie.202503846 by Kobe University, Wiley Online Library on [09/06/2025]. See the Terms and Conditions (https://onlinelibrary.wiley.com/terms-and-conditions) on Wiley Online Library for rules of use; OA articles are governed by the applicable Creative Commons License

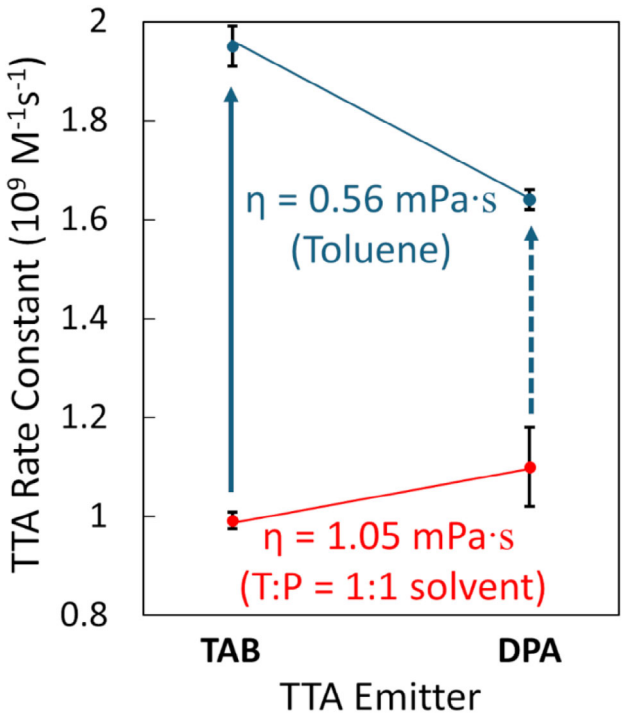


Figure 3. Viscosity effects of k_{TTA} for TAB and DPA emitters. Enhanced TTA is identified by the longer solid arrow in TAB.

results of least squares fittings to determine the τ_T and β values those of which are shown in these figures.

Figure 2c and d show the excitation light intensity dependence of β in the PtOEP/TAB and PtOEP/DPA samples, respectively. We found that there is a nonlinear relationship between β and excitation light intensity. Here, β is expressed by Equation (2):[43]

$$\beta = \frac{2k_{TTA}[^3Emi^*]_0}{(1/\tau_T) + 2k_{TTA}[^3Emi^*]_0} \quad (2)$$

The β value ranges from 0 to 1, and $\beta/2$ equals to the Φ_{TTA}. Solid red curves in Figure 2c and d are the results of least squares fittings using Equations (1) and (2), and k_{TTA} values of TAB and DPA shown in these figures are determined, respectively.

The estimated k_{TTA}s of both samples were on the order of 10^9 ($M^{-1}s^{-1}$). These values are of the same order of magnitude as those of previously reported intermolecular TTA systems in solution.[15,20,45,46] From the blue plots in Figure 3, the k_{TTA} value of TAB was 1.2 times higher than that of DPA. The k_{TTA} value can be dependent of the molecular diffusion rate and of the TTA reaction distance, that is, the spatial extent of the electron density distribution in the triplet state. The diffusion-controlled reaction rate constant (k_d) can be described as depending solely on the solvent viscosity (η), as shown by Equation (3):[25,47]

$$k_d = \frac{8RT}{3\eta} \quad (3)$$

where R is the gas constant, T is the temperature and η is the viscosity. From this, k_d in toluene is estimated to be 10^{10} $M^{-1}s^{-1}$ using viscosity of $\eta = 0.56$ mPa·s at 298 K[48] and is five times larger than the k_{TTA} values. However, considering the low spin statistical factor ($f = 0.4$) in DPA,[20,49] it can be said that $k_{TTA} = 1.64(\pm 0.02) \times 10^9$ $M^{-1}s^{-1}$ is essentially limited by the diffusion. Therefore, it is difficult to determine the intrinsic TTA-rate of the triplet pairs. That the TTA rate for the TAB system is larger than that of the DPA system however suggests that the effective delocalization of the triplet-exciton in the trimer increases the k_{TTA}.

We also determined the k_{TTA} values in a viscous solvent of a mixture of toluene(T): paraffin(P) = 1:1 (v/v) (Figure S4, Table S2). k_{TTA} of TAB was slightly lower or unchanged from that of DPA, as shown by the red plots in Figure 3. This reduction of k_{TTA} for TAB in the viscous solvent would be caused by prolonging the pseudo-rotational time of the triplet-exciton. We note that this reversal is not explained by the Franck-Condon factor for the TTA (vide infra).

To elucidate the accelerated and deaccelerated k_{TTA}s in TAB at the molecular level from spin-state dynamics of the triplet-exciton, we performed TREPR measurements of the PtOEP/TAB and PtOEP/DPA systems. PtOEP and either TAB or DPA were dissolved in solvents with different viscosities prepared by mixing low viscosity toluene and high viscosity liquid paraffin in various mixing ratios.[50,51] The sample solutions were degassed and sealed in 5 mm quartz EPR tubes. As in the time-resolved emission measurements, a Nd:YAG laser at 532 nm was used for light excitation. Importantly, the triplet state of PtOEP is not detected in the X-band (~ 9.5 GHz) EPR used in this study because of its large zero-field splitting (ZFS) interaction.

There are advantages to performing the EPR measurements under varying viscosity conditions. In high viscosity solutions, the rotation of the molecules is slow enough so that the anisotropy by the ZFS is observed with the random orientations. As a result, the motional narrowing effect on the EPR line-shape is suppressed, and EPR spectra similar to those obtained in frozen solutions are observed, allowing for determination of ZFS parameters: D and E.[52,53] As the viscosity of the solvent decreases, the degrees of freedom related to molecular motion, including rotation and vibrations, are increased. This leads to a high rotation frequency of the molecule comparable to the frequency of the ZFS interaction. Thermally activated intramolecular exciton hopping driven by the molecular vibrations may also induce pseudo-rotation as a temperature dependent process. These exciton dynamics can be observed as the motional narrowing effects on the EPR spectral line-shapes.[54]

Figure 4 shows the TREPR spectra of PtOEP/TAB system and PtOEP/DPA system in solvents of varying viscosity at room temperature. Spectral line shapes reflect the spin populations of the triplet sublevels ($|T_+\rangle$, $|T_0\rangle$, $|T_-\rangle$) of emitters, by the TET from PtOEP. Thermal equilibrium electron spin population according to the Boltzmann distribution is assumed here to interpret the microwave-absorptive EPR spectra, although the absorptive spin polarization could possibly be created by the spin-selective reactions in the triplet-pairs during the TTA process, as reported previously.[55] The slower rise and longer decay time of the EPR signal with increasing

© 2025 The Author(s). Angewandte Chemie International Edition published by Wiley-VCH GmbH

15213773, 0, Downloaded from https://onlinelibrary.wiley.com/doi/10.1002/anie.202503846 by Kobe University, Wiley Online Library on [09/06/2025]. See the Terms and Conditions (https://onlinelibrary.wiley.com/terms-and-conditions) on Wiley Online Library for rules of use; OA articles are governed by the applicable Creative Commons License

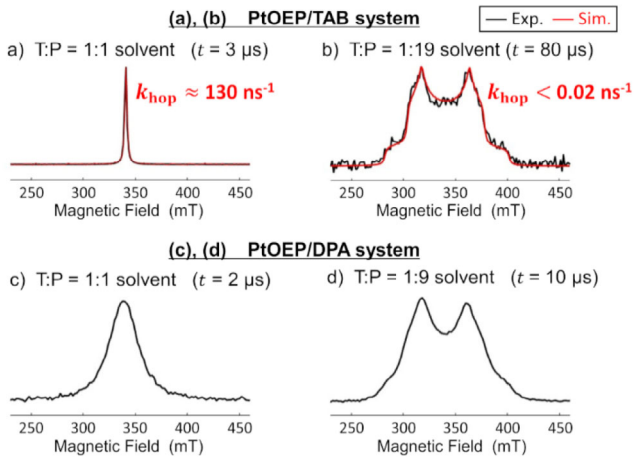


Figure 4. TREPR spectra at the delay time (t) when the microwave absorption intensity reaches maximum under different viscosity conditions. T:P denotes the mixed volume ratio of toluene (T) and liquid paraffin (P). 60 μM PtOEP and 1.2 mM TAB were prepared in (a) with T:P = 1:1 solvent. 35 μM PtOEP and 0.9 mM TAB were prepared in (b) with T:P = 1:19 solvent. 70 μM PtOEP and 2 mM DPA were prepared in (c) T:P = 1:1 solvent and (d) T:P = 1:9 solvent. Red lines in (a) and b) represent the simulation results by the analysis considering the hopping rate (k_{hop}) in Figure 5.

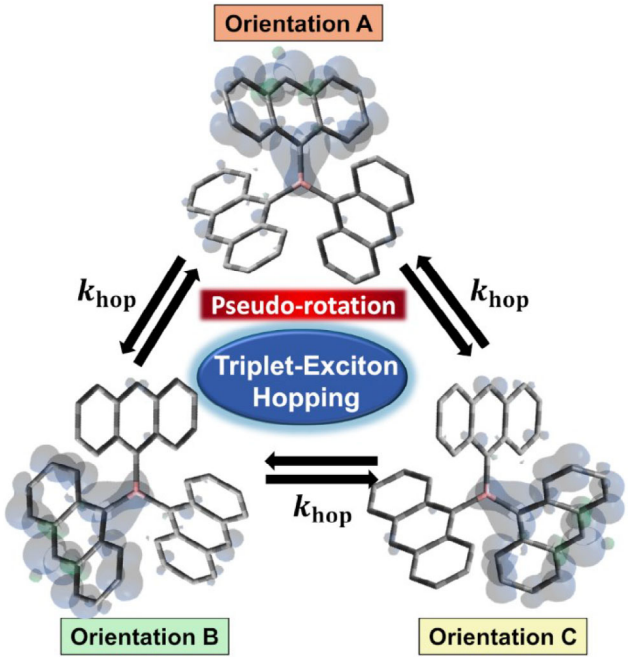


Figure 5. Schematic representation of intramolecular triplet-exciton hopping (pseudo-rotation) between three equivalent sites. The spin density distribution of the triplet-exciton of TAB was obtained from the DFT calculation, as shown with a contour at 0.0024 au.

viscosity is attributed to the slower rate of TET and TTA, respectively, due to slower molecular diffusion.

In PtOEP/TAB system (Figures 4a, S5–S7), the EPR linewidth was narrowed in the mixture of toluene(T): paraffin(P) = 1:1 (v/v) solvent due to a rapid change in the orientation of triplet-exciton relative to the external magnetic field. In contrast, in the T:P = 1:19 solvent, the narrowing effect is suppressed, and broad EPR spectra were observed due to the anisotropy of the spin-spin dipole interaction (Figure 4b). In the T:P = 1:9 mixture of the PtOEP/DPA system (Figure 4d), the motional narrowing is suppressed, as well as in the PtOEP/TAB system with T:P = 1:19. In these viscous solutions, the total splitting widths of the spectra (c.a.120 mT) by the fine structures are comparable for both TAB and DPA. The spin density is distributed to approximately one, locally excited (LE) anthracene in TAB, as in DPA (Figures 5, S8). The similarity of the spin distribution means that the ZFS parameter in DPA is similar to those in TAB, which is consistent with the similar widths by the dipolar splitting in Figure 4b and d, although a motional narrowing effect on the spectrum would slightly influence the line shape.

Comparing the EPR spectra between Figure 4a and c in the T:P = 1:1 solvent, the linewidth of the EPR spectrum of the PtOEP/TAB system is about 3 mT (Figure 4a), while the linewidth of the EPR spectrum of the PtOEP/DPA system is about 30 mT (Figure 4c). This small linewidth for the TAB system should originate from the narrowing effect due to more rapid rotational motions of triplet-exciton of TAB than that of DPA in the presence of the magnetic field, because the ZFS couplings were similar in the viscous media. Typically, molecules with small molecular radii are expected to rotate quickly, leading to more prominent motional narrowing effects. The quick rotation of triplet-excitons on the TAB is thus due to the pseudo-rotation rather than molecular rotation. Therefore, we hypothesize that the intramolecular triplet-exciton hopping occurs within TAB[17,32–34] and thus contributes to the enhanced k_{TTA}. On the other hand, we surmise that the 30 mT width in Figure 4c is caused by the molecular rotation diffusion in ^{3}DPA* because no exciton hopping is expected at the dilute DPA concentration in the fluid.

The spin density distribution of the triplet-exciton of TAB is shown in Figure 5, which is predicted by geometry optimizations as detailed in Figure S11. Since the three anthracene moieties of TAB are arranged in a 3D orthogonal relationship, the hopping causes three orientations of the triplet-exciton to rotate approximately by 90° about two of the axes (x, y, z) within a coordinate frame in the molecule (Figure 5). Such a conformation jump in the orientation of the triplet-exciton leads to motional narrowing of the EPR spectra as the pseudo-rotation, which is effectively equivalent to molecular rotation.[27–29,32,54–56]

Given that the conformation distortion by the local exciton residence is minor (Figure S9b) and thus symmetry of the TAB molecule is approximately preserved due to its trimeric structure, it is expected that there are three equivalent sites where the triplet-exciton is distributed, and we assumed that the triplet-exciton hops between these sites (orientations A, B and C) at the hopping rate constant "k_{hop}".[55,56] Details are described in the Supporting Informational on the EPR spectrum analysis using the coupled stochastic-Liouville equations (SLE) considering the A⇄B, B⇄C, and C⇄A jumps by k_{hop} in the rotating frame with Figures S10–S15 and Tables S3–S6. Validities of the fitting parameters are examined as detailed in Table S6 and Figures S16–S18.

© 2025 The Author(s). Angewandte Chemie International Edition published by Wiley-VCH GmbH

15213773, 0, Downloaded from https://onlinelibrary.wiley.com/doi/10.1002/anie.202503846 by Kobe University, Wiley Online Library on [09/06/2025]. See the Terms and Conditions (https://onlinelibrary.wiley.com/terms-and-conditions) on Wiley Online Library for rules of use; OA articles are governed by the applicable Creative Commons License

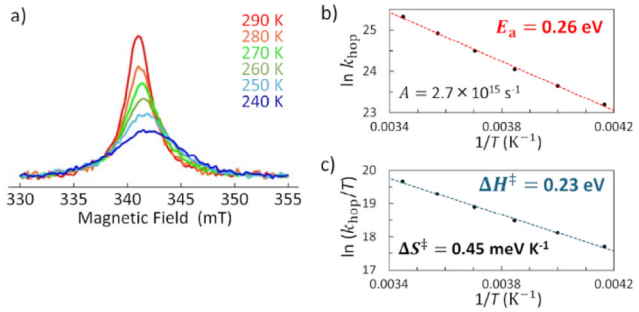


Figure 6. a) TREPR spectra at various temperatures for PtOEP/TAB system in the T:P = 1:1 solvent. EPR spectra are shown for the delay time at which the EPR signal reaches its maximum at each temperature, and the slight shift in the resonant magnetic field by temperature is attributed to the shift in the microwave frequency. Temperature dependence analysis of k_{hop} by b) Arrhenius plot based on Equation (4) and c) Eyring plot based on Equation (5) where $\kappa = 1$ is assumed.

The results of the line shape analyses by the above SLE are shown in Figure 4 where the k_{hop} values for TAB are described. k_{hop} = 130 ns^{-1} in the bulky ^{3}TAB* molecule suggests that the rotation of triplet excitons is due to intramolecular exciton hopping in a much shorter timescale than the molecular rotation dynamics observed in the small molecule of ^{3}DPA*. As the molecular rotation of DPA is suppressed by increasing viscosity (Figure 4d), the k_{hop} value of TAB is also small in the T:P = 1:19 solvent (Figure 4b), indicating that the intramolecular exciton hopping is hindered. The reason for this hinderance is detailed in Figure S9b.

To better elucidate the nature of the intramolecular triplet-exciton hopping in TAB on the activation processes in TTA-UC, we examined the temperature dependence of the EPR spectra. TREPR measurements of the PtOEP/TAB system were conducted (Figure 6a) in the T:P = 1:1 solvent from 240 to 290 K. k_{hop} values were determined by the line shape analysis (Figure S15). In this temperature range, where TET from PtOEP proceeds efficiently, the EPR spectra of TAB are prominently influenced by the motional narrowing, resulting in a single peak at all temperatures. The temperature dependence of k_{hop} for each system was analyzed using the Arrhenius equation of Equation (4) and the Eyring equation, Equation (5):

$$\ln k_{hop} = -\frac{E_a}{k_B T} + \ln A \tag{4}$$

$$\ln \frac{k_{hop}}{T} = -\frac{\Delta H^{\ddagger}}{k_B}\frac{1}{T} + \frac{\Delta S^{\ddagger}}{k_B} + \ln \frac{\kappa k_B}{h} \tag{5}$$

where E_a is the activation energy, k_B is the Boltzmann constant, A is the frequency factor, $\Delta H^{\ddagger}$ is the activation enthalpy, $\Delta S^{\ddagger}$ is the activation entropy and "κ" is the transmission coefficient. E_a = 0.26 eV is determined from the Arrhenius plot (Figure 6b). This activation is associated with the reorganization required for the molecular framework change between the anthracene units (Figure S9b). We also performed the Eyring plot in Figure 6c to determine the activation enthalpy ($\Delta H^{\ddagger}$ = 0.23 eV) and the activation entropy ($\Delta S^{\ddagger}$ = 0.45 meV K^{-1}).

The reorganization energy (λ_T) for the conformation change from the T_1-optimized geometry to the S_0 conformation is obtained as follows:

$$\lambda_T = E_{TS0} - E_{Topt} \tag{6}$$

where E_{TS0} is the total energy of the T_1 state at the S_0 geometry and E_{Topt} for the T_1-optimized geometry. From the computation using the DFT method, λ_T = 0.40 eV is obtained (See Figure S11). The S_1 state exhibits the delocalized CT character (Figure S1), whereas the T_1 state possesses the LE character. A large reorganization energy is also expected on the conformation change from the localized T_1 exciton to the S_1, as well as λ_T = 0.4 eV. $\lambda_T > \Delta H^{\ddagger}$ indicates that the symmetrical S_0 conformation (Figure S9a) is not the transition state for the pseudo-rotation. The positive activation entropy of $\Delta S^{\ddagger}$ = 0.45 meV K^{-1} also represents the highly disordered conformation in the transition state. Asymmetric low-frequency vibration modes are likely to play an important role on the activation for the intramolecular exciton hops. The LE character in the T_1 will avoid the resonance between the central atom and the chromophores by the CT, preserving instability of the single bonds to boron. This results in the highly disordered conformation motions in the transition state, contributing to the positive activation entropy for the pseudo-rotation. This is theoretically confirmed by comparing the triplet character of tri(9-anthryl)amine, as detailed in Figure S19.

The free energy change (ΔG_{TTA}) for the TTA is evaluated to be − 0.9 eV using $\Delta G_{TTA} = E(S_1) - 2E(T_1)$ in Figure 1b. The reorganization energy of λ (= $2\lambda_T$) for $T_1 + T_1 \rightarrow S_0 + S_1$ is estimated to be > 0.80 eV by which conformations of two of the triplet excitons are rearranged to those of the two singlets. From $\Delta G_{TTA} + \lambda \approx 0$ eV, a large Franck-Condon factor is conclusive, as detailed in the Supporting Information. Thus, in the present exergonic TTA systems, the rate constant of k_{TTA} is limited both by the molecular diffusion and by spin statistics, especially in the PtOEP/TAB system.

This suggests that the larger k_{TTA} in TAB compared to DPA may originate from enhancement of the electron exchange between the triplet excitons due to the entropy-driven activation to induce TTA (TTA-ON in Figure 7). Contrary to this, TTA rate constant is expected to be reduced when the activated hopping is frozen because the triplet spin-density distributions are localized to cause mismatches in the electron exchange at the T-T collision (TTA-OFF in Figure 7). In toluene, $1/k_{hop}$ of TAB is estimated to be 1.7 ps (Figure S20) at 298 K. Then, we have calculated a time duration ($t_{collision}$) for two ^{3}TAB* molecules being in contact on a single collision in toluene. It is known that the rate of TTA decreases drastically as the center-to-center distance between the TTA emitters becomes 1 Å longer.[57,58] Based on this, given that the spin-spin exchange integral decays by exp(− αr) with α = 10 nm^{-1}, one can assume that the TTA reaction occurs while the two TAB molecules are within a 0.1 nm variation (Δr) at the distance of the T-T collision. Therefore, $t_{collision}$ can be estimated as the residence time required for a ^{3}TAB*

© 2025 The Author(s). Angewandte Chemie International Edition published by Wiley-VCH GmbH

15213773, 0, Downloaded from https://onlinelibrary.wiley.com/doi/10.1002/anie.202503846 by Kobe University, Wiley Online Library on [09/06/2025]. See the Terms and Conditions (https://onlinelibrary.wiley.com/terms-and-conditions) on Wiley Online Library for rules of use; OA articles are governed by the applicable Creative Commons License

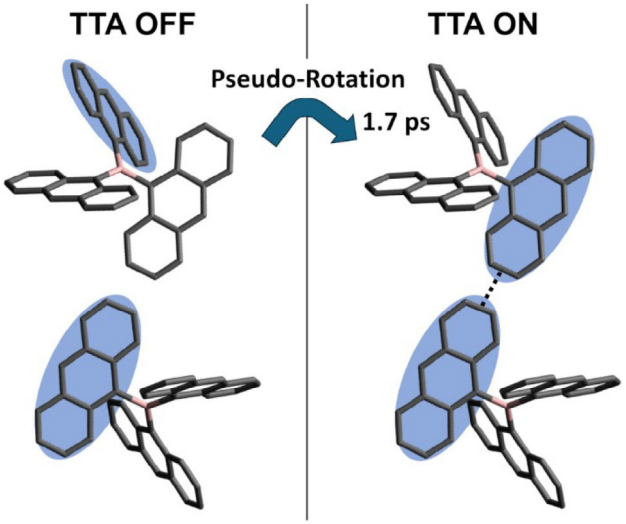


Figure 7. Encounter model of the triplet pairs in TAB. Spin density distributions are represented by the blue ovals. The TTA does not proceed in the left panel because of mismatched orbital configurations for the electron exchange at the encounter. The TTA proceeds when the orbital overlap (dashed line) occurs by the pseudo-rotation in the right panel, resulting in the enhanced TTA.

molecule to diffuse at $\Delta r = 0.1$ nm displacement. Since TAB molecules undergo Brownian motion in three-dimensional space, the mean square displacement (d) can be expressed as follows[59]:

$$d = \sqrt{6D\tau} \tag{7}$$

where D is the diffusion coefficient and τ is the diffusion time. D is estimated by using the Stokes-Einstein equation ($D = k_B T/6\pi\eta r$). In this, d and τ correspond to the Δr and $t_{collision}$, respectively. D in toluene is estimated to be 7.8×10^{-10} m^2 s^{-1} at 298 K. Thus, $t_{collision} = 2.1$ ps is obtained to be comparable to τ_{hop} ($= 1/k_{hop}$) $= 1.7$ ps.

This means that the intramolecular exciton hopping avoids the mismatches at the collision distance, resulting in the TTA reaction rate being close to the diffusion-controlled rate. In contrast, the excitons are not able to change their orientation within the collision time of 2 ps in ^{3}DPA*.

Contrary to the 2 ps hopping time of ^{3}TAB* in toluene, $t_{collision} \ll \tau_{hop} = 8$ ps is obtained in the viscous solvent ($\eta = 1.05$ mPa) in Table S7. This supports the hopping-mediated TTA in toluene ($\eta = 0.56$ mPa) with $t_{collision} = \tau_{hop}$, because $k_{TTA}(^3\text{TAB*}) < k_{TTA}(^3\text{DPA*})$ (red plots of Figure 3) denotes that the inhibited hopping results in the mismatch in the exchange interaction between the ^{3}TAB* molecules to reduce k_{TTA} significantly. The larger increase in $k_{TTA}(^3\text{TAB*})$ as shown by the solid arrow in Figure 3 than the increase represented by the dashed arrow is thus rationalized by the enhanced k_{TTA} by the quick vibronic hopping in ^{3}TAB*.

From this, we conclude that the picosecond intramolecular hopping impacts k_{TTA} in the low viscous solution by expanding effective triplet spin distribution in the time scale of the molecular collision. These ultrafast hopping dynamics can be applicable for several solid-state materials and encapsulated emitter systems to enhance the TTA-UC processes. The weakness of TAB as a TTA emitter is its short triplet lifetime (46.2 μs), which will reduce the chance of the TTA given that the bimolecular k_{TTA} rate constant is not highly influenced due to the diffusion-controlled limit in fluid. Our future task is to enhance k_{TTA} further by designing bulky TTA emitters that lengthen $t_{collision}$, which competes with the vibronic hopping, and to develop TTA emitters with extended triplet lifetime while maintaining the improved k_{TTA}.

Conclusion

In this study, we focused on accelerating the TTA rate constant, which has not been extensively studied before, by synthesizing a trimeric UC emission material, TAB. This material combines three anthracene molecules, which are expected to exhibit intramolecular triplet exciton hopping. We developed a TTA-UC material by combining TAB with one of the photosensitizers, PtOEP, and experimentally evaluated the TTA rate constant and the mobility of triplet excitons during the TTA-UC process using time-resolved luminescence measurements and time-resolved EPR measurements. We confirmed that the structural fluctuations driven by vibronic interactions in the TAB molecule facilitate the quick intramolecular migration of triplet excitons generated by the energy transfer reaction from PtOEP among the anthracene units on TAB, effectively increasing the TTA reactivity. The present picosecond vibronic motion is realized by introducing the asymmetric motions by a localized triplet exciton via the boron atom in TAB. The challenge is to develop new molecules that achieve both extended triplet lifetimes and TTA reaction distances by modifying molecular designs such as introducing substituents. This new strategy of utilizing trimeric molecules that induce long-distance intermolecular TTA is promising to accelerate the development of TTA-UC materials with high light-to-energy conversion efficiency.

Supporting Information

The authors have cited additional references within the Supporting Information.[60,61]

Acknowledgements

This work was partially supported by JSPS KAKENHI Grant-in-Aid for Transformative Research Areas, "Dynamic Exciton (Area No. 20A201)" (JP20H05832) and Grant Nos. JP25H00903, JP23H00309, JP22H00344, JP23H03945E, JP23K17901, JP22K14648 and the JST-CREST Program (JPMJCR23I6). Y.K. and C.K. are grateful for support from Invitational Fellowships for Research in Japan (No. 1201456) by J.S.P.S. Y.K. and E.S. thank to Prof. Seigo Yamauchi (Tohoku University, deceased) on preliminary discussions of the exciton properties in TAB.

© 2025 The Author(s). Angewandte Chemie International Edition published by Wiley-VCH GmbH

15213773, 0, Downloaded from https://onlinelibrary.wiley.com/doi/10.1002/anie.202503846 by Kobe University, Wiley Online Library on [09/06/2025]. See the Terms and Conditions (https://onlinelibrary.wiley.com/terms-and-conditions) on Wiley Online Library for rules of use; OA articles are governed by the applicable Creative Commons License

Conflict of Interests

The authors declare no conflict of interest.

Data Availability Statement

The data that support the findings of this study are available on request from the corresponding author. The data are not publicly available due to privacy or ethical restrictions.

Keywords: Electron paramagnetic resonance · Intramolecular triplet-exciton hopping · Photon upconversion · Triplet-triplet annihilation

[1] T. N. Singh-Rachford, F. N. Castellano, *Coord. Chem. Rev.* **2010**, *254*, 2560–2573.
[2] J. Zhou, Q. Liu, W. Feng, Y. Sun, F. Li, *Chem. Rev.* **2015**, *115*, 395–465.
[3] T. F. Schulze, T. W. Schmidt, *Energy Environ. Sci.* **2015**, *8*, 103–125.
[4] V. Gray, D. Dzebo, M. Abrahamsson, B. Albinsson, K. Moth-Poulsen, *Phys. Chem. Chem. Phys.* **2014**, *16*, 10345–10352.
[5] T. Yu, Y. Liu, Y. Zeng, J. Chen, G. Yang, Y. Li, *Chem. - Eur. J.* **2019**, *25*, 16270–16276.
[6] L. Huang, W. Wu, Y. Li, K. Huang, L. Zeng, W. Lin, G. Han, *J. Am. Chem. Soc.* **2020**, *142*, 18460–18470.
[7] C. Wohnhaas, V. Mailander, M. Droge, M. A. Filatov, D. Busko, Y. Avlasevich, S. Baluschev, T. Miteva, K. Landfester, A. Turshatov, *Macromol. Biosci.* **2013**, *13*, 1422–1430.
[8] O. S. Kwon, H. S. Song, J. Conde, H. I. Kim, N. Artzi, J. H. Kim, *ACS Nano* **2016**, *10*, 1512–1521.
[9] A. W. Punjabi, X. Wang, A. E.-R. Tokatli-Apollon, H. Lee, Y. Zhang, C. Wang, Z. Liu, E. M. Chan, C. Duan, G. Han, *ACS Nano* **2014**, *8*, 10621–10630.
[10] J. Zhao, S. Sun, X. Li, W. Zhang, S. Gou, *ACS Appl. Bio Mater.* **2020**, *3*, 252–262.
[11] Y. Sasaki, M. Oshikawa, P. Bharmoria, H. Kouno, A. Hayashi-Takagi, M. Sato, I. Ajioka, N. Yanai, N. Kimizuka, *Angew. Chem., Int. Ed.* **2019**, *58*, 17827–17833.
[12] M. Uji, J. Kondo, C. Hara-Miyauchi, S. Akimoto, R. Haruki, Y. Sasaki, N. Kimizuka, I. Ajioka, N. Yanai, *Adv. Mater.* **2024**, *36*, e2405509.
[13] A. Olesund, J. Johnsson, F. Edhborg, S. Ghasemi, K. Moth-Poulsen, B. Albinsson, *J. Am. Chem. Soc.* **2022**, *144*, 3706–3716.
[14] C. Ye, V. Gray, J. Martensson, K. Borjesson, *J. Am. Chem. Soc.* **2019**, *141*, 9578–9584.
[15] A. Olesund, S. Ghasemi, K. Moth-Poulsen, B. Albinsson, *J. Am. Chem. Soc.* **2023**, *145*, 22168–22175.
[16] T. Miyashita, P. Jaimes, A. Mardini, M. Fumanal, M. L. Tang, *J. Phys. Chem. Lett.* **2023**, *14*, 6119–6126.
[17] M. Kanoh, Y. Matsui, K. Honda, Y. Kokita, T. Ogaki, E. Ohta, H. Ikeda, *J. Phys. Chem. B* **2021**, *125*, 4831–4837.
[18] A. Monguzzi, R. Tubino, F. Meinardi, *Phys. Rev. B* **2008**, *77*, 155122.
[19] S. H. Lee, M. A. Ayer, R. Vadrucci, W. Weder, Y. C. Simon, *Polym. Chem.* **2014**, *5*, 6898–6904.
[20] A. Olesund, V. Gray, J. Martensson, B. Albinsson, *J. Am. Chem. Soc.* **2021**, *143*, 5745–5754.
[21] C. H. Mulyadi, M. Uji, B. Parmar, K. Orihashi, N. Yanai, *Precis. Chem.* **2024**, *2*, 539–544.
[22] T. N. Singh-Rachford, F. N. Castellano, *J. Phys. Chem. A* **2008**, *112*, 3550–3556.
[23] V. M. Bjelland, H. Nakashima, N. Hashimoto, S. Seo, T. B. Melø, M. Lindgren, *ChemPhotoChem* **2023**, *7*, e202300064.
[24] Y. Sun, L. Wei, S. Zhu, P. Jin, C. He, Q. He, C. Yang, W. Wu, *Sens. Actuators, B* **2023**, *387*, 133764.
[25] Y. Murakami, T. Ito, A. Kawai, *J. Phys. Chem. B* **2014**, *118*, 14442–14451.
[26] Y. Murakami, H. Kikuchi, A. Kawai, *J. Phys. Chem. B* **2013**, *117*, 5180–5187.
[27] M. Bennati, A. Grupp, M. Mehring, *J. Chem. Phys.* **1995**, *102*, 9457–9464.
[28] C. A. Steren, H. V. Willigen, K.-P. Dinse, *J. Phys. Chem.* **1994**, *98*, 7464–7469.
[29] S. Ceola, L. Franco, C. Corvaja, *J. Phys. Chem. B* **2004**, *108*, 9491–9497.
[30] J. L. Dunn, I. D. Hands, C. A. Bates, *J. Mol. Struct.* **2007**, *838*, 60–65.
[31] M. Terazima, K. Sakurada, N. Hirota, H. Shinohara, Y. Saito, *J. Phys. Chem.* **1993**, *97*, 5447–5450.
[32] S. Yamauchi, A. Takahashi, Y. Iwasaki, M. Unno, Y. Ohba, J. Higuchi, A. Blank, H. Levanon, *J. Phys. Chem. A* **2003**, *107*, 1478–1485.
[33] S. Wallin, J. Davidsson, J. Modin, L. Hammarström, *J. Phys. Chem. A* **2005**, *109*, 4697–4704.
[34] M. E. Moret, I. Tavernelli, M. Chergui, U. Rothlisberger, *Chem. - Eur. J.* **2010**, *16*, 5889–5894.
[35] S. Noimark, E. Salvadori, R. Gòmez-Bombarelli, A. J. MacRobert, I. P. Parkin, C. W. M. Kay, *Phys. Chem. Chem. Phys.* **2016**, *18*, 28101–28109.
[36] N. Kitamura, E. Sakuda, *J. Phys. Chem. A* **2005**, *109*, 7429–7434.
[37] S. Yamaguchi, S. Akiyama, K. Tamao, *J. Am. Chem. Soc.* **2000**, *122*, 6335–6336.
[38] K. Yokoyama, Y. Wakikawa, T. Miura, J.-i. Fujimori, F. Ito, T. Ikoma, *J. Phys. Chem. B* **2015**, *119*, 15901–15908.
[39] F. Laquai, G. Wegner, C. Im, A. Busing, S. Heun, *J. Chem. Phys.* **2005**, *123*, 074902.
[40] F. N. Castellano, C. E. McCusker, *Dalton Trans.* **2015**, *44*, 17906–17910.
[41] S. K. Chattopadhyay, C. V. Kumar, P. K. Das, *Chem. Phys. Lett.* **1983**, *98*, 250–254.
[42] F. Edhborg, A. Olesund, B. Albinsson, *Photochem. Photobiol. Sci.* **2022**, *21*, 1143–1158.
[43] S. M. Bachilo, R. B. Weisman, *J. Phys. Chem. A* **2000**, *104*, 7711–7714.
[44] Y. Y. Cheng, B. Fückel, T. Khoury, R. G. C. R. Clady, M. J. Y. Tayebjee, N. J. Ekins-Daukes, M. J. Crossley, T. W. Schmidt, *J. Phys. Chem. Lett.* **2010**, *1*, 1795–1799.
[45] T. N. Singh-Rachford, F. N. Castellano, *Inorg. Chem.* **2009**, *48*, 2541–2548.
[46] F. Deng, J. Blumhoff, F. N. Castellano, *J. Phys. Chem. A* **2013**, *117*, 4412–4419.
[47] N. J. Turro, V. Ramamurthy, J. C. Scaiano, *Principles of Molecular Chemistry: An Introduction*, University Science Books, Sausalito, CA, **2009**.
[48] D. R. Lide, *Handbook of Organic Solvents*, CRC PRESS, Boca Raton, **1995**.
[49] D. G. Bossanyi, Y. Sasaki, S. Wang, D. Chekulaev, N. Kimizuka, N. Yanai, J. Clark, *JACS Au* **2021**, *1*, 2188–2201.
[50] A. Yamauchi, K. Tanaka, M. Fuki, S. Fujiwara, N. Kimizuka, M. Saigo, T. Ryu, K. Onda, R. Kimizuka, N. Ueno, H. Sato, Y. Kobori, K. Miyata, Y. Yanai, *Sci. Adv.* **2024**, *10*, eadi3147.
[51] S. Nakamura, H. Sakai, H. Nagashima, M. Fuki, K. Onishi, R. Khan, Y. Kobori, N. V. Tkachenko, T. Hasobe, *J. Phys. Chem. C* **2021**, *125*, 18287–18296.
[52] R. L. Taylor, D. Housley, M. Barter, A. Porch, K. Whiston, A. Folli, D. M. Murphy, *Catal. Sci. Technol.* **2022**, *12*, 5274–5280.
[53] A. Clark, J. Sedhom, H. Elajaili, G. R. Eaton, S. S. Eaton, *Concepts Magn. Reson. Part A* **2018**, *45A*, e21423.

© 2025 The Author(s). Angewandte Chemie International Edition published by Wiley-VCH GmbH

15213773, 0, Downloaded from https://onlinelibrary.wiley.com/doi/10.1002/anie.202503846 by Kobe University, Wiley Online Library on [09/06/2025]. See the Terms and Conditions (https://onlinelibrary.wiley.com/terms-and-conditions) on Wiley Online Library for rules of use; OA articles are governed by the applicable Creative Commons License

[54] H. Sillescu, *J. Chem. Phys.* **1971**, *54*, 2110–2119.
[55] T. Okamoto, S. Izawa, M. Hiramoto, Y. Kobori, *J. Phys. Chem. Lett.* **2024**, *15*, 2966–2975.
[56] Y. Han, M. Hamada, I. Y. Chang, K. Hyeon-Deuk, Y. Kobori, Y. Kobayashi, *J. Am. Chem. Soc.* **2021**, *143*, 2239–2249.
[57] R. Sato, H. Kitoh-Nishioka, K. Kamada, T. Mizokuro, K. Kobayashi, Y. Shigeta, *J. Phys. Chem. C* **2018**, *122*, 5334–5340.
[58] R. Sato, H. Kitoh-Nishioka, T. Yanai, Y. Shigeta, *Chem. Lett.* **2017**, *46*, 873–875.
[59] A. Einstein, *Investigations on the Theory of the Brownian Movement*, Dover Publications, New York, **1956**.
[60] S. Richert, B. Limburg, H. L. Anderson, C. R. Timmel, *J. Am. Chem. Soc.* **2017**, *139*, 12003–12008.
[61] L. E. McNamara, A. Zhou, T. Rajh, L. Sun, J. S. Anderson, *Cell Rep. Phys. Sci.* **2023**, *4*, 101693.

Manuscript received: February 16, 2025
Revised manuscript received: May 17, 2025
Accepted manuscript online: May 19, 2025
Version of record online: ■■, ■■

© 2025 The Author(s). Angewandte Chemie International Edition published by Wiley-VCH GmbH

15213773, 0, Downloaded from https://onlinelibrary.wiley.com/doi/10.1002/anie.202503846 by Kobe University, Wiley Online Library on [09/06/2025]. See the Terms and Conditions (https://onlinelibrary.wiley.com/terms-and-conditions) on Wiley Online Library for rules of use; OA articles are governed by the applicable Creative Commons License